A NEW ACTIVE POWER PHOTOVOLTAIC SYSTEM FOR RESIDENTIAL APPLICATIONS

Saša Sladić[1*] – David Nedeljković[2]

[1] Department of Electric Power Systems, Faculty of Engineering, University of Rijeka, Croatia
[2] Department of Mechatronics, Faculty of Electrical Engineering, University of Ljubljana, Slovenia

ARTICLE INFO

***Article history*:**
Received: 31.01.2017.
Received in revised form: 12.06.17.
Accepted: 12.06.17.

Keywords:
Single-phase active power filter
Boost power converter
Efficiency considerations
Photovoltaic systems

Abstract:

In this paper, a single-phase parallel (shunt) active power filter (APF), operating with adaptive filter capacitor voltage (AV), is used as a base for combined approach to active power filtering and to connection of additional voltage sources to AC network. Through filter capacitor voltage adaptation, improvement of switching conditions can be observed both from AC and DC side of active power filter, making this approach suitable for connection of low-voltage DC sources (30 – 100 V) to AC network. Thus, advantages are provided for application of emerging solar cells technologies (e.g. thin-film), which operate in this voltage range. Furthermore, improvement can be noticed in sense of power factor correction as the primary role of APF. In this paper, there are various connections of DC sources through an additional converter for filter capacitor voltage adaptation discussed and evaluated. Active power photovoltaic systems performances are verified by simulations and by measurements.

1 Introduction

DC voltage from photovoltaics or other DC sources can be inverted to AC network through DC-link voltage of a single-phase parallel active power filter. Thus, the active power filter (APF) acquires yet another function, besides compensation of reactive power and harmonic distortion of nonlinear loads, supplied by AC network. Since efficiency is an important parameter in renewable energy applications, an additional buck converter is used commonly in utilization of APFs as a link between a photovoltaic source and the AC network [1, 2]. In order to achieve proper operation of active power filter, filter capacitor voltage has to be higher than maximum line voltage, and consequently, it is necessary to connect large number of solar cells in series [1, 3] in order to achieve appropriate DC link voltage. Commercial solutions, based on APF with boost converter, are flexible because of additional step-up of photovoltaic (PV) voltage.

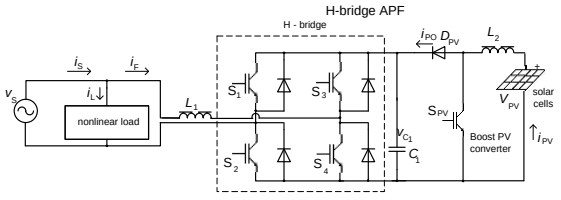

Figure 1. Single-phase shunt active power filter with boost converter and PV source (constant filter capacitor voltage).

[*] Corresponding author. Tel.: ++385 51 651 440
E-mail address: sladics@riteh.hr

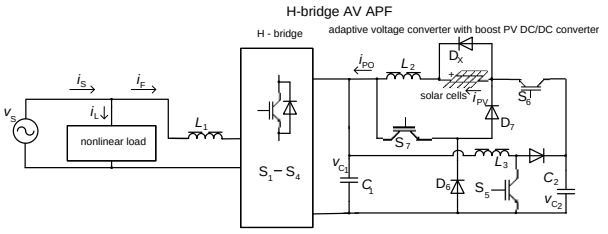

Figure 2. Proposed topology of APF based on boost converter (adaptive filter capacitor voltage).

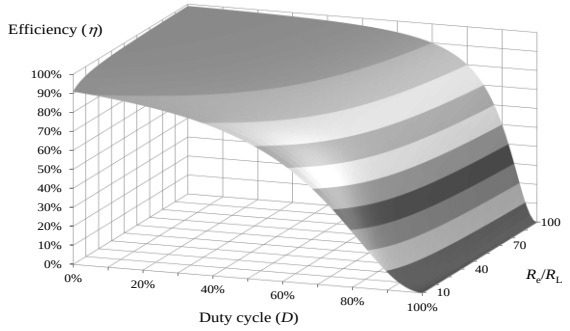

Figure 3. Efficiency of boost converter depends on duty cycle (D) and ratio between equivalent output resistance (R_e) and parasitic resistance (R_L).

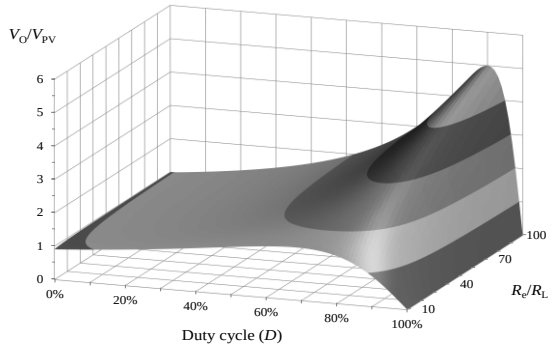

Figure 4. Boost converter voltage step-up ratio (V_O/V_{PV}) depends on duty cycle (D) and ratio between equivalent output resistance (R_e) and parasitic resistance (R_L).

Output voltage of a boost converter connected to solar cells represents filter capacitor voltage of APF [4], which is approximately constant during steady state operation. In this way, functions of APF's compensation and maximum power tracking (MPPT) of solar cells/module are independent, without significant interaction. This approach is quite effective for classical PV modules [1, 2], but it has drawbacks for applications with higher voltage step-up which is common in newer solar cell technologies (e.g. thin-film) [2, 5]. This usually decreases efficiency due to losses on parasitic inductor resistance of the boost converter [3].

At this point, it seems that the use of transformer can solve this problem [4, 5], since the transformers are very efficient components, but they could saturate during operation. The transformer saturation arises especially in push-pull converter [5], but in some other approaches with flyback converter, for instance, magnetic core is not completely utilized, which is another reason for further study of advanced transformerless solutions [6].

It appears that many converters could be incorporated into a larger and more sophisticated converter, where the effect of parasitic inductor resistance could be reduced. Consequently, additional semiconductor switches [7, 8, 9] which control charging and discharging of filter capacitor according to load and AC network conditions [10, 11] are required. Simulations and practical results show the efficiency increase as a consequence of improved switching conditions. Model of classic APF [12] has been extended by different adaptive voltage converter topologies. It is shown, that time utilization of energy flow [13] does not omit an application of different MPPT algorithms [14, 15] ever since a fast microcontroller system has been used [16, 17].

2 Losses and efficiency considerations for boost converter

In order to compare APF with constant (Fig. 1) and adaptive filter capacitor voltage (Fig. 2) concerning their ability to connect additional energy sources, it is useful to introduce equivalent output resistance R_e of applied boost converter, which is defined as ratio between DC/DC converter output voltage V_O (being equal to filter capacitor voltage V_{C1}) and its output current I_{PO}:

$$R_e = \frac{V_O}{I_{PO}} = \frac{V_{PV}}{I_{PO}(1-D)} = \frac{V_{PV}}{I_{PV}(1-D)^2} = \frac{V_{C1}}{I_{PO}}. \quad (1)$$

There, V_{PV} and I_{PV} are solar module voltage and current, respectively. The equation (1) is valid for a continuous boost converter operation (idealized form). It can be noted that higher filter capacitor

voltage V_{C1} requires higher duty cycle D of boost converter. Boost converter application leads to high input currents which are followed by increased losses on parasitic inductor resistances (e.g. resistance R_L of inductor L_2 from Fig. 1 and 2). Efficiency of boost converter could be calculated as a ratio between output power and total power, as follows:

$$\eta = \frac{1}{1+\frac{R_L}{R_e(1-D)^2}} = \frac{1}{1+\frac{R_L \cdot I_{PV} \cdot (1-D)^2}{V_{PV}(1-D)^2}} = \frac{1}{1+\frac{R_L \cdot I_{PV}}{V_{PV}}}. \quad (2)$$

Efficiency therefore decreases with increased parasitic resistance R_L of inductor L_2 and with higher duty cycle D, as represented in Fig. 3. Higher voltage step-up which is needed for low PV voltage applications seems to be very hard to achieve, since converter step-up ratio (V_O/V_{PV}) is not only a function of duty cycle as in an ideal case, but also depends on ratio between equivalent output resistance (R_e) and parasitic resistance (R_L):

$$\frac{V_O}{V_{PV}} = \frac{1}{1-D}\frac{1}{1+\frac{1}{(1-D)^2}\frac{R_L}{R_e}}. \quad (3)$$

Practical consequence of this equation is that boosted PV voltage can't achieve required level by relatively high filter capacitor voltage, regardless of duty cycle *D's* increase (Fig. 4).

3 Losses and efficiency consideration of adaptive voltage active power filter

A combination of two DC/DC converters has to be implemented to provide proper charging and discharging of the filter capacitor, thus obtaining an adaptive voltage waveform on APF filter capacitor. Consequently, the filter capacitor is being charged and discharged for about few hundred volts during a single half-cycle of line voltage, therefore its capacitance has to be much lower than in the case of constant voltage DC-link capacitor – typical capacitance of adaptive voltage filter capacitor is 10 μF or less. Recharging of such low capacitance will not contribute significantly to converter losses; even more, slight efficiency improvement, compared to constant filter capacitor voltage approach can be expected due to improved switching conditions in H-bridge APF [9, 10]. Filter capacitor voltage V_{C1} should follow its reference value v_{Cr}, which has slightly modified waveform of absolute line voltage:

$$v_{Cr} = k|v_S| + k_1 \cdot i_{fk}, \quad (4)$$

$$i_{fk} = \begin{cases} |i_F|; & v_S \cdot i_F < 0 \\ 0; & v_S \cdot i_F \geq 0 \end{cases}, \quad (5)$$

$$i_f = i_F \cdot \mathrm{sign}(v_S), \quad (6)$$

$$v_{C1} \approx v_{Cr}, \quad (7)$$

where v_S is input voltage, k is a constant around 1, k_1 is a constant with resistive character (around 10 Ω), i_S represents line source current and i_F is filter current, all according to Fig. 1 and 2. Consequently, filter capacitor voltage reaches very low level during the zero-transition of line supply voltage, leading to H-bridge switching conditions close to zero voltage switching (ZVS). Although this phenomenon is not fully implemented, the APF filter capacitor voltage depends on network conditions. Anyhow, in the case of adaptive voltage (AV) APF, the maximum filter capacitor voltage is upwards limited like in constant voltage APF (Fig. 5 a).

4 Simulation results of adaptive voltage approach in active power filtering

APF with adaptive voltage has been simulated with Simplorer simulation software. The switching frequency of APF (basic switching frequency) is 20 kHz. Fig. 5 shows that simulated filter capacitor reference voltage reaches very low voltages for various load current waveforms (i_L). D–class of load current (according to IEC standards) is very suitable for adaptive voltage approach since the intervals of high and low filter capacitor voltage are equally distributed (Fig. 5 a). Oppositely, the square waveform of load current results in relatively short interval of low voltage on filter capacitor (Fig. 5 b). The reference filter capacitor voltage waveforms (v_{Cr}) obtained in Fig. 5 c and Fig. 5 d are also suitable for connecting of low voltage solar cells, since low filter capacitor voltage enables higher PV currents even for low PV voltages (e.g. application of thin-film solar cells modules).

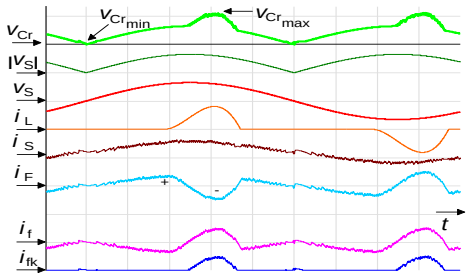

a) D-class load (uncontrolled capacitive rectifier)

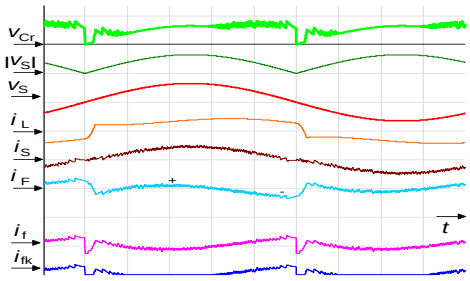

b) Uncontrolled inductive rectifier

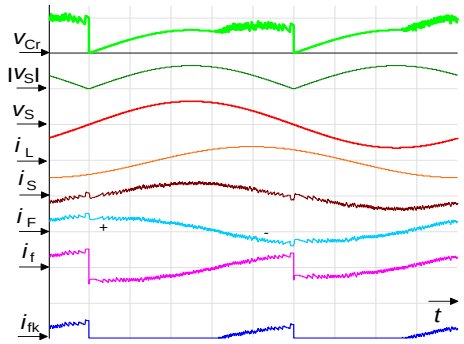

c) Induction machine

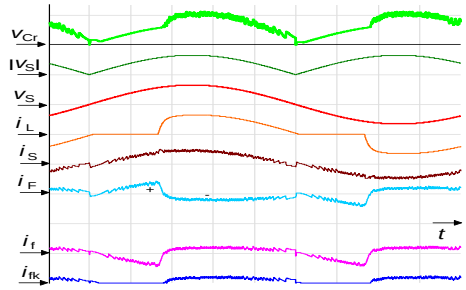

d) A-class load (AC/AC dimmer with RL load)

Figure 5. Simulated generation of adaptive voltage reference v_{Cr} for different load types: absolute value of source voltage Iv_SI, source voltage v_S, load current i_L, source current i_S, filter current i_F, signals i_f and i_{fk}; 500 V/div, 25 A/div, 2 ms/div.

In the next step, an influence of adaptive filter capacitor voltage to connected boost converter was investigated. For simulation, the following parameters were taken into account: P_{PV} = 33 W, p_{MAX}= 83 W, D = 0.8, L_1 = 1 mH, V_{PV} = 33 V, C_1 = 10 μF, $R(L_2)$ = 1 Ω, f_s=10 kHz. According to Fig. 6, energy transfer is possible for lower DC voltages than in the case of constant voltage APF. It can be noted that boost converter could charge filter capacitor only during the short intervals of reduced filter capacitor voltage. Without such intervals energy transfer from the DC source would be prevented according to (2).

5 AV APF steady state experimental results

In order to validate influence of adaptive filter capacitor voltage to boost converter output current, an experimental model based on Texas Instruments TMS320F2407 was used. For adaptive voltage converter, a switching frequency (5 kHz), which is lower than switching frequency of APF (20 kHz) was selected, although much closer tracking of filter capacitor voltage to its reference could be obtained with higher switching frequency of adaptive voltage converter (e.g. 20 kHz). Namely, switching losses of converter rapidly increase with higher switching frequency.

It has been reported earlier [9] about the source current THD improvement using variable filter capacitor voltage approach instead of the constant DC link voltage. The improvement can be measured for all load types [10, 11], but larger improvement occurs for D-class of load (Fig. 5 a). In this case source current with THD of 82 % has been reduced to 7.5 % with classic approach and to 4.9 % with adaptive voltage approach. The results were recorded at 1.2 kW of load power.

In Fig. 8, measured signals for a combination of D-class load and A-class load are presented. Simulation results (Fig. 7) are compared with measured results (Fig. 8), also. Fig. 9 shows efficiency versus active power of load for the constant and adaptive voltage APF. In spite of different waveforms which can be obtained, as filter capacitor voltage reference (Fig. 5 and Fig. 7), efficiency improvement in adaptive voltage APF appears in each case when the difference between minimal and maximal value of filter capacitor voltage v_{C1} is higher than 200 V (Fig 5 a). This is valid for a wide area of different DC link voltages

(400 V – 1 kV); for lower voltages, efficiency improvement could be even higher, because the same switching frequency (5 kHz) allows the filter capacitor to be charged and discharged more precisely.

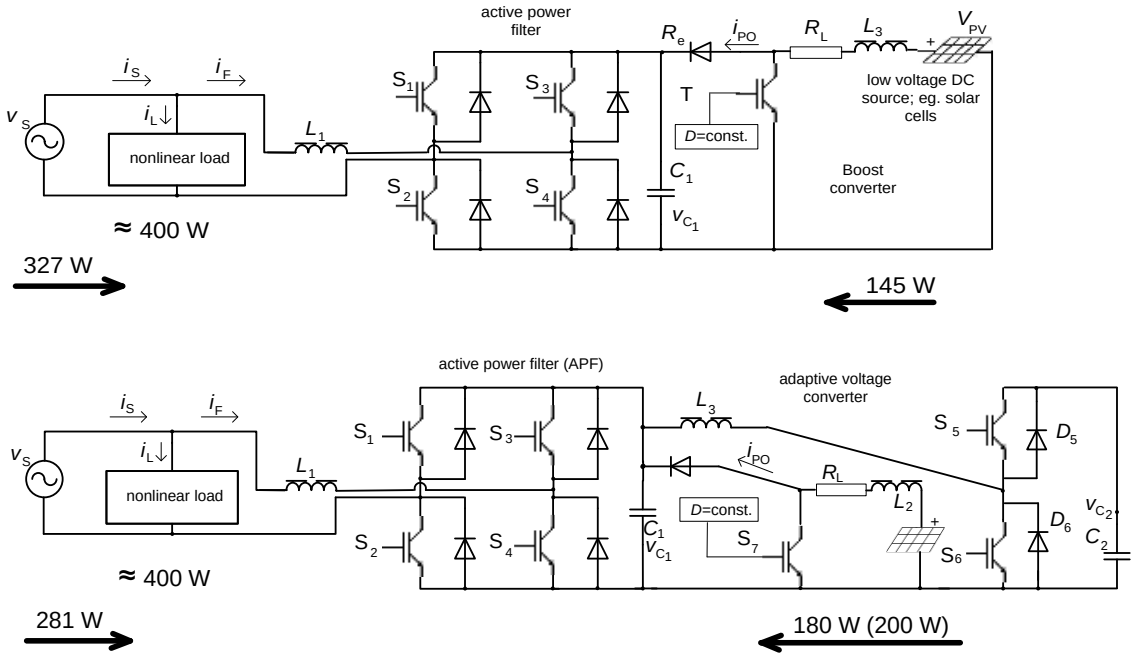

Figure 6. Classic APF (above) and adaptive voltage APF (below) under the same conditions (400 V DC link voltage in classic APF and 400 V maximal v_{C1} in adaptive voltage APF).

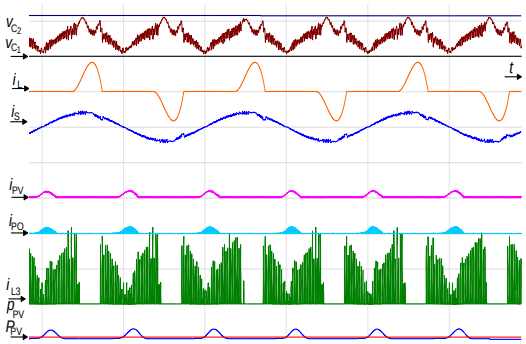

Figure 7. Simulation of APF with adaptive filter capacitor voltage v_{C1}, connected to PV source with boost converter: DC link voltage v_{C2}, load current i_L, source current i_S, DC source current i_{PV}, output current of boost converter i_{PO}, filter capacitor discharging current i_{L3}, instantaneous DC source power (p_{PV}), active power of DC source P_{PV}; 500 V/div, 25 A/div, 2 ms/div, 100 W/div.

6 Synergy between PV energy sources and adaptive voltage APF through Boost Buck Topology

Fig. 6 shows a comparison between AV APF and constant voltage APF concerning their connection to additional DC source - It was measured that more power can be transmitted to capacitor with variable voltage than to constant voltage DC link. Consequently, supply current i_S decreases, leading to lower consumption and higher efficiency.

In interaction of AV APF with boost converter, it was noticed that from the boost converter to the AC side equal power can be transmitted at lower duty cycle D than with constant voltage APF. Thus, higher efficiency is provided for the boost converter. This improvement can be explained by (2), since V_{PV} apparently has a higher value during the intervals of reduced filter capacitor voltage (V_{C1}). Both simulation (Fig 7) and experimental results (Fig 8) show that in spite of the constant duty cycle (optionally MPPT), boost converter

output current (i_{PO}) has impulse waveform which can be biased by some DC component for higher power.

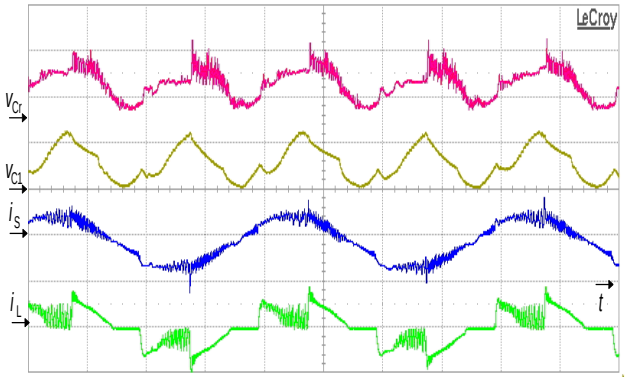

Figure 8. Adaptive filter capacitor voltage reference v_{Cr}, adaptive filter capacitor voltage v_{C1}, line current i_S and load current i_L, recorded for a combination of nonlinear loads; 5 ms/div, 200 V/div, 2 A/div.

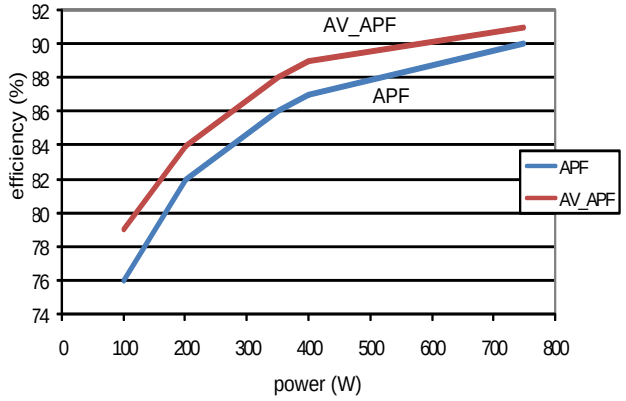

Figure 9. Efficiency versus active power of load for constant and adaptive voltage APF.

For the increased values of boost converter duty cycle, impulse waveform of i_{PO} is still notable, but energy transfer occurs also during the intervals of increased filter capacitor voltage. Anyhow, energy transmitted to the AC side by boost converter, strongly depends on filter capacitor voltage and for higher voltages v_{C1}, power delivery from low voltage DC source (V_{PV} = 33 V) will not be possible at all (neither for AV APF).

There are few topologies [7, 8] which can be used for achieving adaptive filter capacitor voltage. Each of them is suitable for connection of DC sources of different type (e.g. different renewable energy sources, especially for residential applications). Since the PV cells represent a DC source, it is desirable to accomplish a filter capacitor charging (buck converter) and discharging (boost converter) through separate inductors [9, 10].

This can be accomplished by topology, named boost-buck AV APF converter (Fig. 10), which is appropriate for cases when the difference between DC source voltage and DC link voltage is too high both for constant voltage and adaptive voltage approach. Such a converter can transmit energy to AC side even at voltage level of single solar cell (≈1 V). Output current of boost converter (current through L_2) can be expressed as:

$$i_{PO} = \begin{cases} i_{Dx} & P_{PV} = 0 \\ i_{S6} + i_{D6} & P_{PV} > 0 \\ \dfrac{i_{S6}}{D_6} + i_{S7} \cdot \dfrac{(1-D_7)}{D_7} & P_{PV} >> 0 \end{cases} . \quad (8)$$

There, D_6 and D_7 represent duty cycles of switches S_6 and S_7 respectively, and i_{S6} and i_{S7} are corresponding currents. Photocurrent value remains unaffected during the buck converter action and is increased during boost converter action:

$$i_{PV} = \begin{cases} i_{PO} & V_{PV} > 0 \quad \text{buck action} \\ i_{PO} \cdot \dfrac{1}{(1-D_7)} & V_{PV} > 0 \quad \text{boost action} \end{cases} . \quad (9)$$

However, the peak value of output current for low voltages V_{PV} is not limited by its DC source voltage, but with the current through switch S_6 and diode D_6 (continuous operation). In (8) and (9) it was taken into account that the converters (buck and boost) are not active within the same time interval, but their actions support each other in sense of output current i_{PO}.

Fig. 7 shows impulse waveform of DC source current (i_{PO}) when otherwise for constant voltage approach energy transfer from DC to AC side would not be possible (due to high DC link voltage). It can be noted that DC source transmits its energy to filter capacitor and further to the AC network only during intervals of lower filter capacitor voltage or when the switch S_6 conducts. The measurement confirmed simulation results (Fig. 8 and 12).

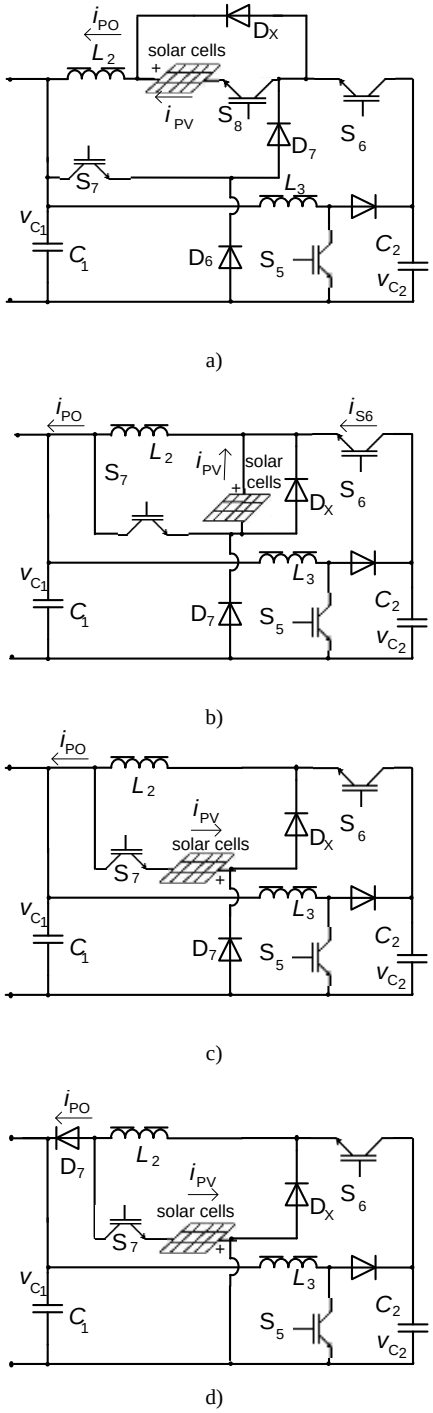

Figure 10. Adaptive voltage (AV) converter with two inductors and PV source connected in different ways.

Sharing the same inductor (L_2) for charging of filter capacitor and boost converter opens various possibilities for connecting a DC source (PV cells) within the same boost-buck topology (Fig. 10). The solution in Fig. 10 a has possibility of reducing the current of switch S_6 in order to achieve MPPT function. Similar topology is presented in Fig. 10 b, where solar cells are connected to flyback diode circuit of boost-buck adaptive voltage converter. That means that a current flowing through the solar cells is lower than in previous example. It could be written:

$$i_{\mathrm{PV}} = \begin{cases} i_{\mathrm{PO}} \cdot (1 - D_6) & V_{\mathrm{PV}} > 0 \quad \text{buck action} \\ i_{\mathrm{PO}} \cdot \dfrac{1}{(1 - D_7)} & V_{\mathrm{PV}} > 0 \quad \text{boost action} \end{cases} . \quad (10)$$

In this case maximal PV current becomes more dependent on load current of APF filter since synergy is reduced compared to (9). In an example from Fig. 10 c solar cells current is completely independent of charging current of capacitor C_1, i.e. if switch S_7 is constantly turned off, current through solar cells remains zero. The solution from Fig. 10 d. differs from Fig. 10 c only in diode positioning.
Each of these topologies is favorable for some specific voltage level, but solution from Fig. 10 a enables highest maximal currents for minimal voltage levels, so it is considered as optimal. It is shown together with APF in Fig. 11 in order to investigate dynamics of AV APF.

7 AV APF dynamics

AV APF has few advantages in sense of dynamics in comparison to the constant voltage H-bridge circuit (Fig. 1). In this circuit, dynamics of APF is influenced by series connection of voltage v_{C2} and PV cells voltage. Therefore, the voltage which is seen from the point of H-bridge inverter is higher than in case of the constant DC link voltage. This is also the case in Fig. 10 a, whenever the switches S_6 and S_8 are closed. This means that solar cells can increase compensating capabilities of classic – constant DC link voltage APF in intervals of rapid load current changes. In this way possible saturation of APF would be avoided. This approach is not limited to AV APF only (Fig. 10 a, 11), but it could be applied to classic APFs. It means that a "two level" converter becomes a "three level converter" by appropriate solar cells connection. More ever, inrush current of capacitor C_1 has been reduced comparing to classic solution (Fig. 1) since its capacitance is decreased to less than 10 μF. Increased flexibility could be described

mathematically by means of filter capacitor voltage v_{C1}.

Operation of AV APF (Fig. 11) can be mathematically described. The supply line voltage (v_S) or its fundamental harmonic component can be used to determine the supply line current reference (i_S):

$$i_S = k_2 \cdot v_S . \tag{11}$$

Constant k_2 represents proportionality factor related with DC link voltage (V_{C2} for AV APF). For a voltage source APF one transistor in transistor leg conducts:

$$S_{S1} + S_{S2} = 1, \tag{12}$$

meaning either the state of switch S_1 or the state of switch S_2 is on. Polarity (sign) of supply line voltage v_S determines switching of transistors S_1 and S_2:

$$S_{S2} = \frac{1+\mathrm{sign}(v_S)}{2}. \tag{13}$$

However, switching of switches S_3 and S_4 is much faster (≈ 20 kHz). It is defined by (11) and characterized by:

$$S_{S3} + S_{S4} = 1, \tag{14}$$

$$v_x = (S_{S2} \cdot S_{S3} - S_{S1} \cdot S_{S4}) \cdot v_{C1}. \tag{15}$$

where the v_x is marked in Fig. 11. The stated equations for AV APF are:

$$\frac{i_F}{dt} = \frac{1}{L_1}\left[v_S - (S_{S2} + S_{S3} - 1) \cdot v_{C1}\right]. \tag{16}$$

$$\frac{v_{C1}}{dt} = \frac{1}{C_1}\left[S_{S2} + S_{S3} - 1\right] \cdot i_F \ . \tag{17}$$

Adaptation of the filter capacitor voltage is closely related with rapid filter current changes (16), as well as decreased value of filter capacitor capacitance (C_1).

Different algorithms could be applied for each topology from Fig 10. For the converter system shown in Fig 11, results are shown in Fig. 12. Switching of transistor S_5 is accomplished with constant duty cycle ($D_5 \approx 0.7$) which is activated when the filter capacitor voltage v_{C1} is higher than its reference. On the other hand, switch S_6 is conducting when the filter capacitor voltage is lower than its reference (4-7). The duty cycle of switch S_6 has been chosen in order to achieve best dynamic response ($D_6 \approx 0.8$). Switching of S_7 implements the MPPT function. In Fig. 12 it is shown that AV APF has fast dynamic response to load current change due to the low capacitance of filter capacitor.

Theoretically, the AV APF system could operate, also for special case of load current where it is obtained a constant filter capacitor voltage, according to (4). In that case the AV APF would have the same waveforms and efficiency like the constant voltage APF, both concerning the AC and DC side of AV APF converter. Such case can be hardly expected especially because of the filter capacitor capacitance minimization (Fig. 12). However, any load current waveform change (from this theoretic case) brings the filter capacitor voltage adaptation, improved switching conditions, and supported PV converter action.

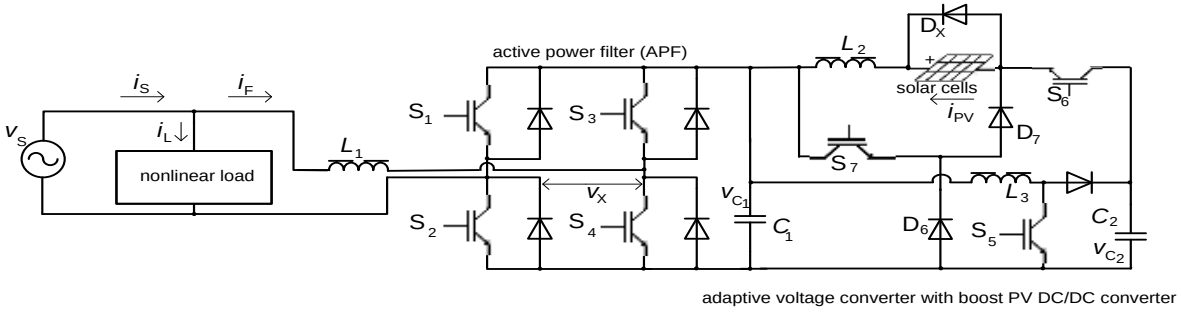

Figure 11. Single-phase shunt active power filter with adaptive filter capacitor voltage with two inductors in adaptive converter circuit (boost-buck topology).

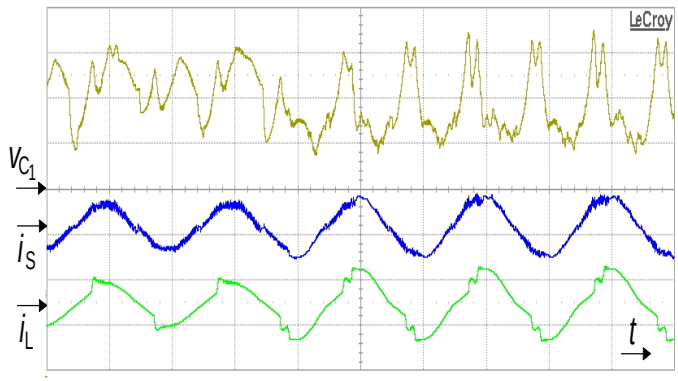

Figure 12. Measured transient recorded for boost-buck AV APF for change of A-class load current i_L; filter capacitor voltage v_{C1}, source.

8 Conclusion

It has been shown that the active power filter with adaptive filter capacitor voltage (AV APF) has slightly higher efficiency (1 %) than the active power filter with constant filter capacitor voltage. Since the filter capacitor voltage waveform in AV APF depends on load current, different filter capacitor voltage waveforms can appear. In spite of the fact that each such case (waveform) has its particular losses and efficiency, numerous measurements show that efficiency improvement appears always when the difference between minimal and maximal filter capacitor voltage is higher than 200 V (for DC link voltage above 400 V). Several topologies were compared in order to recharge the filter capacitor in synergy with the low-voltage photovoltaic sources (33 V). Besides, adaptation of the filter capacitor voltage brings an improvement in sense of line current harmonic distortion with minor dynamic performance improvement compared to constant DC link voltage APF.

References

[1] Chen, Y., Smedley, K. M.: *A Cost-effective single-stage inverter with maximum power point tracking*, IEEE Transactions on Power Electronics, vol. 19, no. 5, pp. 1289-1294, September 2004.

[2] Wu, T. F., Nien, H. S., Shen, C. L., Chen, T. M.: *A Single-Phase Inverter System for PV Power Injection and Active Filtering With Nonlinear Inductor Consideration*, IEEE Transactions on Industry Applications, Vol. 41, no. 4, pp. 1075-1083, July/August 2005.

[3] Walker, G. R., Sernia, P. C.: *Cascaded DC-DC Converter Connection of Photovoltaic Modules*, IEEE Transactions on Power Electronics, Vol. 19, no. 4, pp. 24-29, July 2004.

[4] Kjær, S. B., Pedersen, J. K., Blaabjerg, F.: *A Review of Single-Phase Grid-Connected Inverters for Photovoltaic Modules*, IEEE Transactions on Industry Applications, Vol. 41, no. 5, pp. 1292-1306, September/October 2005.

[5] Wang, J., Peng, F. Z. Anderson, J. Joseph, J. Buffenbarger, R.: *Low Cost Fuel Cell Converter System for Residential Power Generation*, Transactions on Power Electronics, vol. 19, no. 5, September 2004.

[6] Dah-Chuan, Lu, D., Agelidis, V. G.: *Photovoltaic-Battery-Powered DC Bus System for Common Portable Electronic Devices*, IEEE Letters on Power Electronics, Vol. 24, no. 3, March 2009.

[7] Behera, S., Das, S.P., Doradla, S.R.: *Quasi-resonant inverter-fed direct torque controlled induction motor drive*, Electric power System Research, vol. 77, pp. 946-955, June 2007.

[8] Divan, D. M., Skibinski, G.: *Zero-switching-loss inverters for high-power applications*, IEEE Transactions on Industry Applications, vol. 25, no. 4, July/August 1989.

[9] Sladić, S., Barišić, B., Soković, M.: *Cost-effective power converter for thin film solar cell technology and improved power quality*, Journal of Materials Processing Technology, vol. 201, pp. 786-790, May 2008.

[10] Sladić, S., Zajec, P., Nedeljković, D.: Transformerless connections of low voltage DC sources to single-phase shunt active power filter with adaptive filter capacitor voltage, *Speedam*, Pisa, Italy, 2010.

[11] Sladić**,** S., Skok, S., Nedeljković, D.: Efficiency considerations and application limits of single-phase active power filter with converters for photoenergy applications, International Journal of Photoenergy vol. 2011, Article ID 643912, 8 pages, doi:10.1 55/2011/643912, 2011.

[12] Torrey, D., Al-Zamel, A. M. A. M.: *Single-Phase Active Power Filters for Multiple Nonlinear Loads*, IEEE Trans. on Power Electronics, vol. 10, no. 3, May 1995.

[13] Perinić, M., Mikac, T., Maričić, S.: *Optimizing Time Utilization of FMS*, Strojarstvo vol. 50, 2008.

[14] Leyva, R., Olalla, C., Zazo, H., Cabal, C., Cid-Pastor, A., Queinnec, I., Alonso, C.: *MPPT based on sinusoidal extremum-seeking control in PV generation*, International Journal of Photoenergy, vol. 2012.

[15] Andrejašič, T., Jankovec, M., Topič, M.: *Comparison of direct maximum power point tracking algorithms using EN 50530 dynamic test procedure*, Renewable Power Generation, IET, Vol. 5, issue 4, pp. 281-286, July, 2011.

[16] Sumina, D., Bulić, N., Mišković, M., *Application of a DSP-based control system in a course in synchronous machines and excitation systems*, International Journal of Electrical Engineering Education, vol. 49, issue: 3 Special Issue: SI pp: 334-348, July 2012.

[17] Štimac, G., Braut, S., Bulić, N., Žigulić, R.: M*odeling and experimental verification of a flexible rotor/AMB system*, COMPEL – The International Journal for Computation and Mathematics in Electrical Engineering, vol. 32, issue: 4, pp: 1244-1254, 2013.